Biophysical Chemistry 159 (2011) 100–109

Contents lists available at ScienceDirect

Biophysical Chemistry

journal homepage: http://www.elsevier.com/locate/biophyschem

A bifunctional allosteric site in the dimer interface of procaspase-3

Joshua L. Schipper [a], Sarah H. MacKenzie [a], Anil Sharma [b,1], A. Clay Clark [a,*]

[a] Department of Molecular and Structural Biochemistry, North Carolina State University, Raleigh, NC 27695, USA
[b] Department of Chemistry, North Carolina State University, Raleigh, NC 27695, USA

ARTICLE INFO

Article history:
Received 30 March 2011
Received in revised form 17 May 2011
Accepted 17 May 2011
Available online 25 May 2011

Keywords:
Caspase
Apoptosis
Allosteric activator
Drug design
Cancer therapy

ABSTRACT

The dimer interface of caspase-3 contains a bifunctional allosteric site in which the enzyme can be activated or inactivated, depending on the context of the protein. In the mature caspase-3, the binding of allosteric inhibitors to the interface results in an order-to-disorder transition in the active site loops. In procaspase-3, by contrast, the binding of allosteric activators to the interface results in a disorder-to-order transition in the active site. We have utilized the allosteric site to identify a small molecule activator of procaspase and to characterize its binding to the protease. The data suggest that an efficient activator must stabilize the active conformer of the zymogen by expelling the intersubunit linker from the interface, and it must interact with active site residues found in the allosteric site. Small molecule activators that fulfill the two requirements should provide scaffolds for drug candidates as a therapeutic strategy for directly promoting procaspase-3 activation in cancer cells.

1. Introduction

1.1. Caspases and apoptosis

It is estimated that 10^{10} cells are produced each day in a healthy adult human. In order to maintain homeostasis, the same number of cells is removed, either by apoptosis or autophagy [1–3]. Apoptosis is a tightly regulated process of cell suicide that is carried out by a family of cysteinyl aspartate-specific proteases called caspases. All caspases are produced initially as inactive zymogens and must undergo maturation to yield the active protease. Initiator caspases, such as caspases-8 and -9, are activated after formation of signaling complexes, such as the DISC (death inducing signaling complex) or the apoptosome [4,5], in so-called extrinsic or intrinsic activation pathways, respectively. Initiator caspases activate the effector procaspase-3, which is then transformed into caspase-3, the executioner of apoptosis. For a review of caspase activation pathways, see Boatright and Salvesen [6].

1.2. Caspase structures and allostery

Structurally, caspases are homodimers of heterodimers, where each heterodimer contains a large and small subunit of about 18 and 12 kDa, respectively. Because the heterodimer is one structural unit consisting of a six-stranded β-sheet core with five α-helices on the protein surface and a single active site, it is referred to here as the monomer. The dimer interface is formed by an approximate 180-degree rotation of two monomers such that the dimer contains a twelve-stranded β-sheet core with two active sites on nearly opposite sides of the protein (Fig. 1A). In the procaspase form, the subunits within the monomer are covalently connected by a linker, called the intersubunit linker or IL, which binds in the dimer interface and maintains the procaspase in an inactive conformation. In the cell, activation of initiator procaspases results from dimerization of an inactive monomer either via the DISC or the apoptosome. In contrast, effector procaspases are stable dimers and are activated by cleavage of the intersubunit linker. With procaspase-3, for example, cleavage of D175 by initiator caspases results in the reordering of several active site loops, caused by the release of the IL from binding in the interface. Importantly, the substrate binding loop, called L3, moves from a solvent exposed position to form a groove on the protein surface. Following chain cleavage, the IL (now called L2') from one monomer interacts with the active site of the second monomer to stabilize the active conformer (Fig. 1A).

While the conformational changes resulting in caspase activation have been described elsewhere [6–9], several events related to the studies presented here are noted. Upon formation of the active site, the substrate binding loop (L3) is stabilized through interactions in the dimer interface. In caspase-3, for example, R164, which is adjacent to the catalytic C163 on active site loop 2 (L2), moves from a solvent exposed position into the interface where the side-chain intercalates between Y197, and P201 from L3 (Fig. 1B). The positive charge is neutralized by E124, located on a loop above the interface. The close

* Corresponding author at: Department of Molecular and Structural Biochemistry, 128 Polk Hall, North Carolina State University, Raleigh, NC 27695-7622, USA. Tel.: +1 919 515 5805; fax: +1 919 515 2047.
E-mail address: clay_clark@ncsu.edu (A.C. Clark).
[1] Current address: Envigen Pharmaceuticals, 2 Davis Drive, Research Triangle Park, NC 27709, USA.

0301-4622/$ – see front matter © 2011 Elsevier B.V. All rights reserved.
doi:10.1016/j.bpc.2011.05.013

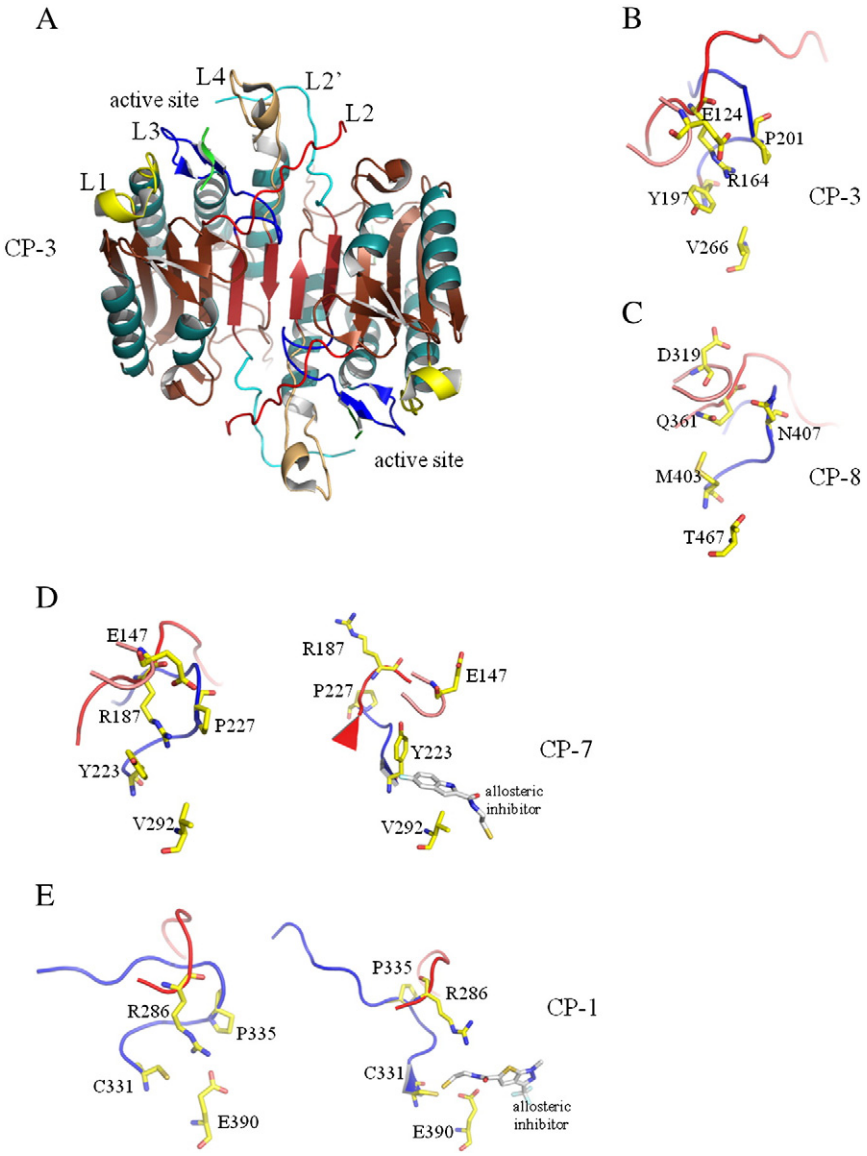

Fig. 1. Caspase structure and active site loops. (A) Structure of caspase-3 showing the two active sites and five active site loops — L1 (yellow), L2 (red), L3 (blue), L4 (brown), L2' (cyan). Note that loops from only one active site are labeled. (B) Caspase-3 active site arginine intercalated in dimer interface. (C) Caspase-8 interactions of Q361 in dimer interface. (D) Active caspase-7 (left panel) demonstrating intercalation of active site arginine in dimer interface, and allosterically inhibited caspase-7 (right panel). (E) Active caspase-1 (left panel) demonstrating salt bridge between active site arginine and dimer interface glutamate, and allosterically inhibited caspase-1 (right panel). For panels B–E, V266 (caspase-3), T467 (caspase-8), V292 (caspase-7) and E390 (caspase-1) represent equivalent sites in the dimer interface. Figures were generated using Pymol and the following structure files: caspase-3: 2J30, caspase-8: 1QTN, caspase-7 (active): 1F1J, caspase-7 (inhibited): 1SHL, caspase-1 (active): 2HBQ, caspase-1 (inhibited): 2FQQ.

homologue, caspase-7, has similar interactions (Fig. 1D, left), as does the inflammatory caspase-1 (Fig. 1E, left). In the case of caspase-1, however, the arginine side-chain from L2 forms a salt-bridge with E390, which in caspases-3 and -7 is a valine. Overall, the themes are similar in that intercalation of the arginine that is near the catalytic cysteine is stabilized by electrostatic and/or π-electron–electrostatic interactions. These interactions between the arginine and amino acids in the interface stabilize the catalytic cysteine in the active conformation. In contrast to the inflammatory and effector caspases, initiator caspases use a different mechanism for activation. In caspase-8, for example, the active site arginine found in other caspases is replaced with glutamine (Q361), which H-bonds to the backbone carbonyl of D319 on a loop above the interface (Fig. 1C). At present, it is not clear how the contacts in caspase-8 affect active site stability.

The interactions of the active site loops with the dimer interface represent an allosteric network that stabilizes the active site. Mutational studies of caspase-1 show that the two active sites are connected through the R286-E390 salt bridge, where the glutamates from each monomer also interact through a water molecule at the center of the protein [10,11]. Allosteric inhibitors of caspases-1 and -7 have been described [11,12], and while the details of binding differ, the overall effect is similar. One observes that binding of the compound in the interface results in a disordered active site. The substrate binding loop (L3) is unable to insert into the dimer interface due to steric clashes with the inhibitor (Fig. 1D and E, right panels). Consequently, the stabilizing interactions do not form with the active site arginine from L2. Overall, the allosteric inhibitors destabilize the active conformer in favor of an inactive conformer with disordered active site loops.

1.3. General model of caspase conformational dynamics

We have shown recently that the procaspase-3 dimer also fluctuates between two states, one resembles the inactive conformer and the other resembles the active conformer [13]. A mutation of V266 to glutamate in the dimer interface results in expulsion of the IL from the interface, thus destabilizing the inactive conformer in favor of the active conformer in a mechanism similar to that described above for the cleaved protein. In addition, the IL of the constitutively active procaspase-3 was not cleaved, demonstrating that activation can occur even in the absence of chain cleavage. One difference between the active procaspase and the fully mature protein (that is, the cleaved caspase-3) is that L2' remains covalently attached in the IL of the procaspase, so it is unavailable to interact completely with the active site of the second monomer. As a result, the activity of the active procaspase conformer is lower than that of the mature caspase by about five folds. However, it possesses sufficient activity to kill cells efficiently [13]. In a broader sense, the intrinsic conformational dynamics may be a general feature of dimeric procaspases. Salvesen and colleagues have shown that the active site of the procaspase-8 dimer can be ordered in the presence of kosmotropes [14,15].

Based on collective data from a number of studies, we suggest the general models shown in Fig. 2. Initiator procaspases are inactive monomers until induced to form dimers by death scaffolds (*in vivo*) or other factors such as kosmotropes (*in vitro*) (Fig. 2A). The equilibrium constant between monomer and dimer has been estimated to be in the low micromolar range, so the monomer is favored *in vivo* [15,16], but the equilibrium appears to favor the active conformer once the dimer forms. We note that the relative population of active to inactive dimer may differ for different initiator procaspases; whereas procaspase-9 appears to be fully active on the apoptosome [17], the procaspase-8 dimer may require chain cleavage for full activity [18].

In contrast, the dimer is favored in solution for effector procaspases (Fig. 2B), where the equilibrium constant between monomer and dimer has been estimated to be in the low nanomolar range [19]. In addition, the relative population of inactive to active dimer favors the inactive conformer. So, controlling the activities of initiator or effector procaspases through dimerization or active site rearrangements, respectively, provides tight control over apoptosis. Cleavage of the IL results in irreversible maturation, and it leads to a new equilibrium between inactive and active mature caspases (Fig. 2). For effector caspases, the inactive conformer is favored, where L2' remains bound in the interface similar to its position in the procaspase [20,21], but the active conformer is stabilized in the presence of substrate.

The important concept of the conformational dynamics of the pro- and mature caspase dimers is that similar transitions occur between the inactive and active conformers, as described above. The same allosteric site that was shown to inhibit the mature caspase also was shown to activate the procaspase. The common theme appears to be an order-to-disorder transition in the case of inhibition, or a disorder-to-order transition in the case of activation. Thus the allosteric site in the interface is bifunctional, where the inhibitor or activator selects the appropriate state from the ensemble of native states. Because of the conformational dynamics, shown in Fig. 2 and described above, a small drug compound, in principle, needs only to stabilize the active conformer of procaspase-3 to induce apoptosis.

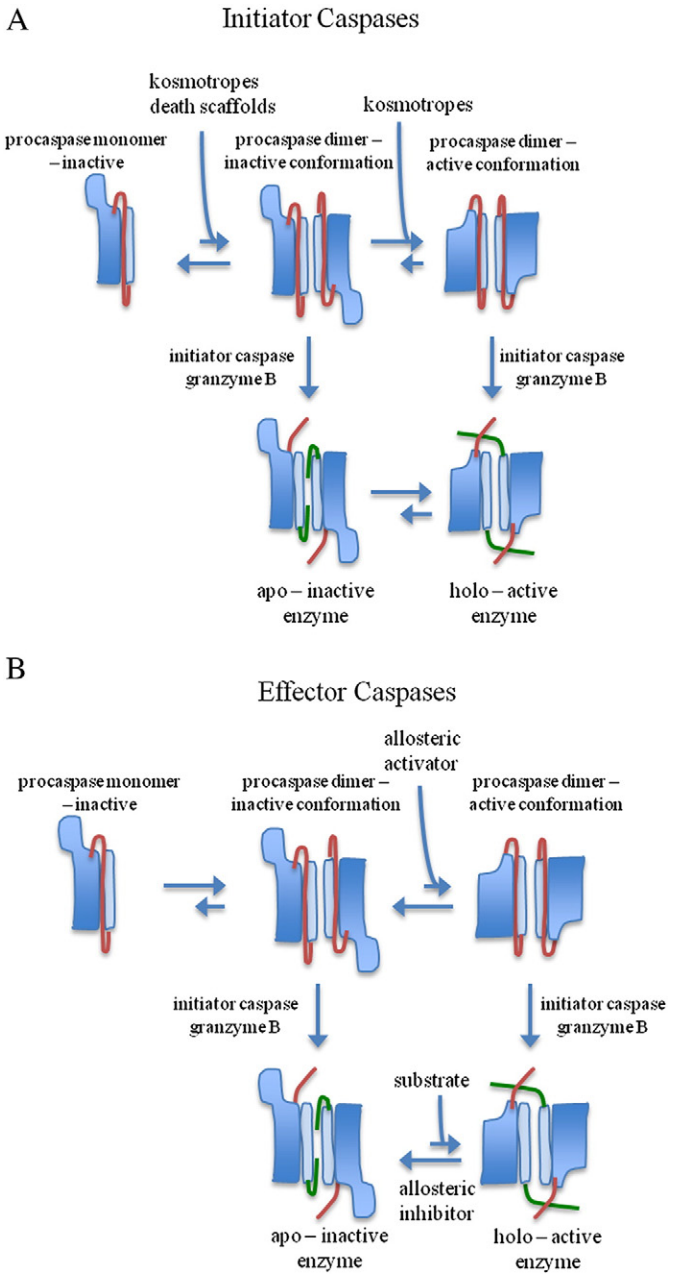

Fig. 2. Common conformational transitions in caspases. For initiator (A) and effector (B) caspases, the inactive monomer forms an inactive dimer, which is in equilibrium with an active procaspase dimer. Dimers of initiator procaspases are facilitated by death scaffolds or kosmotropes, whereas dimers of effector caspases are stable in the absence of external factors. The inactive dimer is favored for effector caspases. Cleavage of the intersubunit linker (red in procaspase; green and red in caspase) results in formation of mature caspase. The cleaved caspase also has multiple states in equilibrium between inactive and active forms. For A and B, blue = large subunit, cyan = small subunit.

1.4. Activating caspases in cancer cells

In 2007, a total of 2,423,712 deaths were registered in the United States (http://www.cdc.gov). Heart disease (616,067 deaths) and cancer (562,875 deaths) account for about half of the total number of deaths, where an estimated $104 billion was spent on cancer care in 2006. For colorectal cancer alone, there were estimated to be about 140,000 new cases and about $7 billion spent on treatment in 2010 [22].

Cancer cells are known to evade proapoptotic signals, and it is well established that anticancer drugs are effective at killing cancer cells by inducing the cell death program [23–25]. Current chemotherapeutic strategies indirectly induce apoptosis by promoting cellular toxicity and DNA damage, and ultimately most therapies result in cell death due to activation of caspase-3 (Fig. 3A). Recent efforts to target the

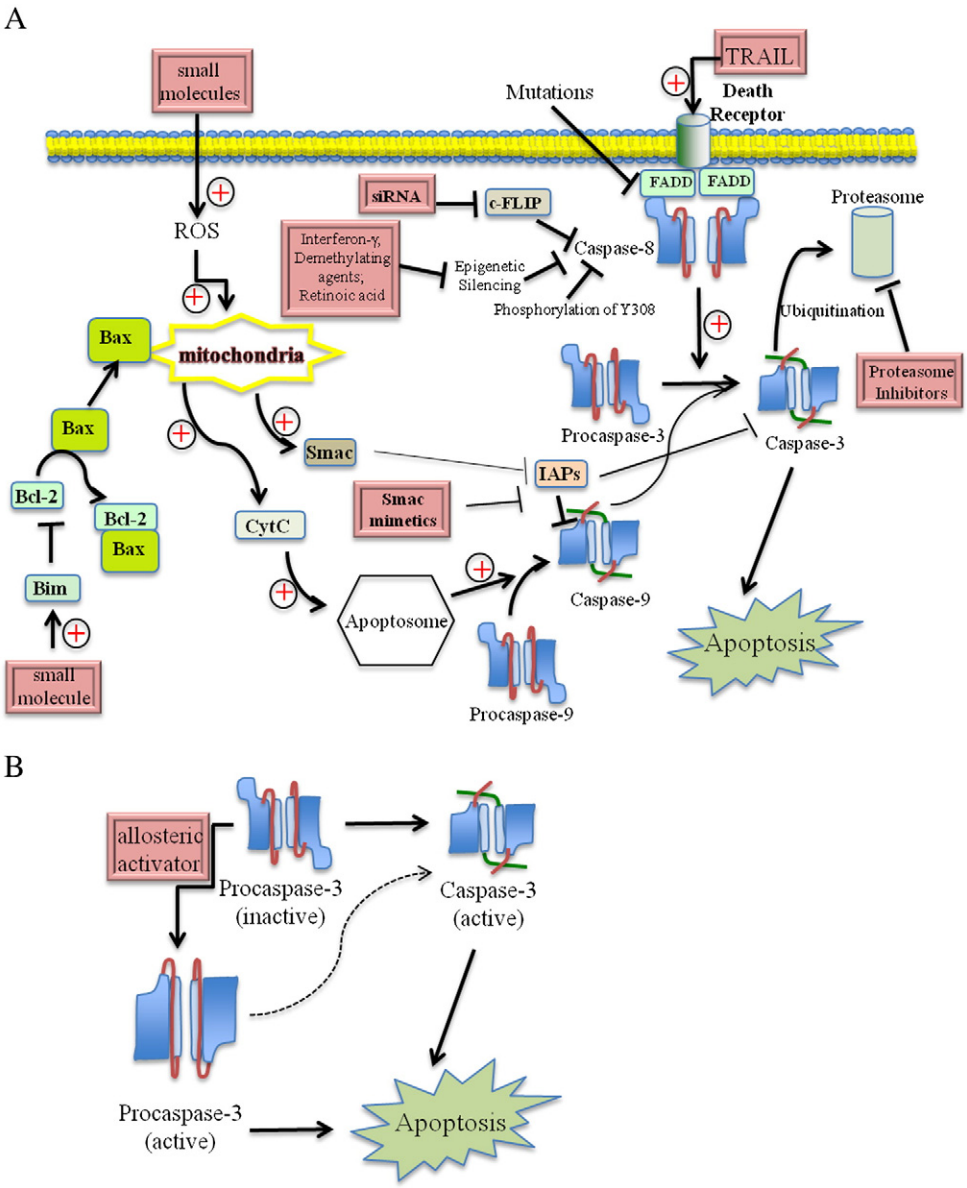

Fig. 3. Therapeutic strategies for activating apoptosis. (A) Intrinsic or extrinsic apoptosis pathways are activated by a variety of mechanisms, as shown in the pink boxes. The therapeutic strategies are described in the text. (B) Allosteric activation of procaspase-3. The active procaspase can carry out apoptosis in the absence of chain cleavage and bypass inhibition by XIAP. The proposed pathway does not rule out maturation of procaspase-3 (dashed line) and apoptosis via the mature protease.

apoptotic machinery as an anti-cancer strategy are focused on reactivating the intrinsic or extrinsic pathways by inhibiting key regulatory proteins involved in apoptosis, namely Bcl-2 family members, XIAP and Smac/Diablo [26]. In addition, several therapies target increased activation of caspase-8, either through increased transcription or through activation of death receptors [27,28], or inhibiting ubiquitin-mediated degradation of apoptotic proteins [29]. One problem with such approaches is that tumorigenic cells can build resistance because the therapies target proteins that have early entry in the apoptotic program [30], so combined approaches generally are used to increase effectiveness. While there is a large pool of inactive procaspase-3 in many cancer cells compared to normal cells [31], currently there is no therapeutic strategy to directly activate procaspase-3. We suggest that utilizing the allosteric site in the dimer interface to target procaspase-3, rather than upstream regulators of apoptosis, could lead to a more effective, direct therapy since activated procaspase-3 is competent to carry out apoptosis and also evades inhibition by XIAP [13] (Fig. 3B).

1.5. Twenty-five years of Gibbs and modern biothermodynamics

A goal of the early Gibbs conference organizers was to develop a broader vision for using thermodynamic techniques to study biological systems [32]. Since its inception, the Gibbs conference has shown that biothermodynamic techniques provide an excellent link between structural biology and molecular/cellular biology by quantifying interactions and providing mechanistic details to structural and functional studies. In the past twenty-five years, the field of biothermodynamics has broadened from single-technique measurements, tabulation of free energies, or counting ATPs hydrolyzed per reaction. Modern biothermodynamic investigations integrate a variety of techniques to examine many aspects of macromolecular

ensembles that are not accessible through examination of static structures or cellular phenotypes. The influence of the Gibbs community on studies of caspase activation is unmistakable. We note that all of the caspase conformational states shown in Fig. 2 currently are not accessible by x-ray crystallography. Considering allostery as the communication among a selection of states within an ensemble, biothermodynamic measurements provide access to the conformational transitions as well as to the effects of ligand binding to the various states of the caspases. Coupling structural and thermodynamic analyses with molecular and cellular biology and computational modeling provides mechanistic details of caspase ensembles that facilitate the drug design efforts described here.

2. Materials and methods

2.1. Docking

Structure files for each molecule were created using the chemical structure drawing tool MarvinSketch 5.3 (ChemAxon, www.chemaxon.com). Docking studies were performed using the DOCK6.3 software package (dock.compbio.ucsf.edu) [33,34]. The molecular modeling program UCSF Chimera 1.4 [35] was used to prepare the receptor (caspase-3, pdb ID 2J30) and ligand files by removing waters, rebuilding missing residues and removing alternate conformations, adding hydrogens, calculating charges, and saving structures in mol2 format. The DOCK6 sphgen tool was used to create receptor spheres with radii between 1.4 Å and 5.5 Å. Spheres within 10 Å of the center of the dimer interface were selected for use in docking simulation, and a grid box was generated extending out 5 Å from the spheres. Docking was performed by incorporating ligand flexibility, and Amber scores were used for analysis.

2.2. Activation assay

Compounds selected for *in vitro* studies were purchased from the Maybridge Screening Library (www.maybridge.com), encompassing a range of predicted binding energies. Each compound was dissolved in DMSO and stored at 4 °C. The effect of these compounds on the activity of uncleavable procaspase-3(D9A,D28A,D175A), called procaspase-3(D_3A) [36], was determined using a Modulus II plate reader (Promega, Sunnyvale, CA). To each well of a black 96-well plate was added 180 μL of assay buffer (150 mM Tris–HCl, pH 7.5, 100 mM DTT, 0.1% CHAPS, 50 mM NaCl, 1% sucrose) containing protein (100 nM final concentration) and compound, where the concentration of each compound ranged from 200 nM to 400 μM. Fluorogenic substrate (Ac-DEVD-AMC) (20 μL of a 200 μM stock) was dispensed into each well so that the final concentration was 20 μM, and the fluorescence emission (410–460 nm) was measured for three minutes following excitation at 365 nm. Activity was determined as the change in relative fluorescence units per second. Each plate also contained controls of procaspase-3(D_3A) without added compound.

2.3. Synthesis of compound 42

Compound 42 (N2,N2-diethyl-5-{5-[(diethylamino)sulfonyl]-2-thienyl}thiophene-2-sulfonamide) was synthesized using a butyllithium reaction, as summarized in Fig. 4D below. 5,5′-dibromo-2,2′-bithiophene (162 mg) was dissolved in 3 mL THF (for ~100 mM concentration) and cooled to −78 °C in a dry-ice/isopropanol bath. n-Butyllithium (~860 μL of 1.6 M) in hexane was added slowly and stirred for 30 min. Sulfur dioxide was bubbled through cold solution for 5 min, and then the precipitated sulphinate salt was filtered onto Whatman filter paper and dried overnight under vacuum. The precipitant was then resuspended in dichloromethane (6 mL) and cooled to −78 °C in a dry-ice/isopropanol bath. Sulfuryl chloride (200 μL) was added slowly, and the solution was incubated for 30 min. Diethylamine (~30 mL) was then added slowly until the pH returned to neutral. The compound was purified using a silica gel column by elution in a solution of ethyl acetate (30%) in hexane after a wash of 100 mL hexane. The product (Fig. 4D, compound 4) was examined by NMR, with the following results confirming the successful synthesis — ^{1}H NMR ($CDCl_3$, δ_{ppm}): 1.2 (t, 12H, J = 7.0 Hz, 4X CH_3), 3.36 (q, 8H, J = 7.0 Hz, 4X CH_2), 7.15 (d, 2H, J = 4 Hz, 2X CH thiophene), 7.45 (d, 2H, J = 4 Hz, 2X CH thiophene). ^{13}C NMR ($CDCl_3$, δ_{ppm}): 14.52, 42.99, 125.05, 132.17, 140.94, 141.04. In addition, the product was examined by ESI ion trap mass spectrometry, and the mass was determined to be 437.07, compared to a calculated mass for product (Fig. 4D, compound 4 — $C_{16}H_{25}N_2O_4S_4$) of 437.06, again confirming the correct product.

2.4. Enzyme activity assay in presence of compound 42

Enzyme activity assays were performed using protocols described previously and the fluorogenic substrate Ac-DEVD-AFC [36,37]. Procaspase-3(D_3A) (400 nM) was incubated in assay buffer containing 400 μM compound. Samples were excited at 400 nm, and the fluorescence emission was measured at 505 nm using a PTI C-61 spectrofluorometer (Photon Technology International, Birmingham, New Jersey).

2.5. Isothermal titration calorimetry of compound 42 binding to caspase-3

Isothermal titration calorimetry was performed on a Microcal Auto-ITC200 microcalorimeter (Piscataway, NJ). Caspase-3(D9A, D28A) was used to measure binding of compound 42. The variant retains the pro-domain and has increased stability compared to wild-type caspase-3, yet it exhibits the same level of activity as wild-type [38]. Protein (50 μM) was in a buffer of 50 mM potassium phosphate, pH 7.2, containing 100 mM DTT and 5% DMSO. The injection sample contained 500 μM compound 42 in the same buffer, and injections (2 μL) were performed for 4 s every two minutes, for a total of 20 injections. The reference sample contained buffer only.

3. Results and discussion

3.1. Molecule selection

A library of 62 molecules was generated for simulated docking with the dimer interface of caspase-3. The molecules were first selected using the online Maybridge Screening Library database (www.maybridge.com). To narrow down the list of compounds, only those molecules that had good drug-like properties according to Lipinski's rules of five [39] were selected. These properties, namely the octanol–water partition coefficient (less than 5), number of hydrogen bond donors (less than 5) or acceptors (less than 10), and molecular weight (less than 500 Da), were assessed for each molecule in the online database. The list was further reduced by including only molecules with the potential for crossing the blood–brain barrier, and with a molecular weight greater than 200 Da. From this set, 62 compounds comprising a variety of functional groups were selected (Supplemental Fig. 1). The selected compounds had a general size and shape that would fit into the cavity of the caspase-3 dimer interface (described below).

Results from the docking studies of the 62 compounds showed that all but five were able to dock to the interface and were scored based on potential binding energies (Fig. 4A). The average AMBER score of the compounds was −23.0 ± 12.8, and scores ranged from ~−60 to ~+6 (the scores represent relative binding energies and have arbitrary units), where the more negative score indicates better binding. In a small pilot study, thirteen of the compounds (Fig. 4B) were tested further for their ability to activate procaspase-3 in *in vitro* activity

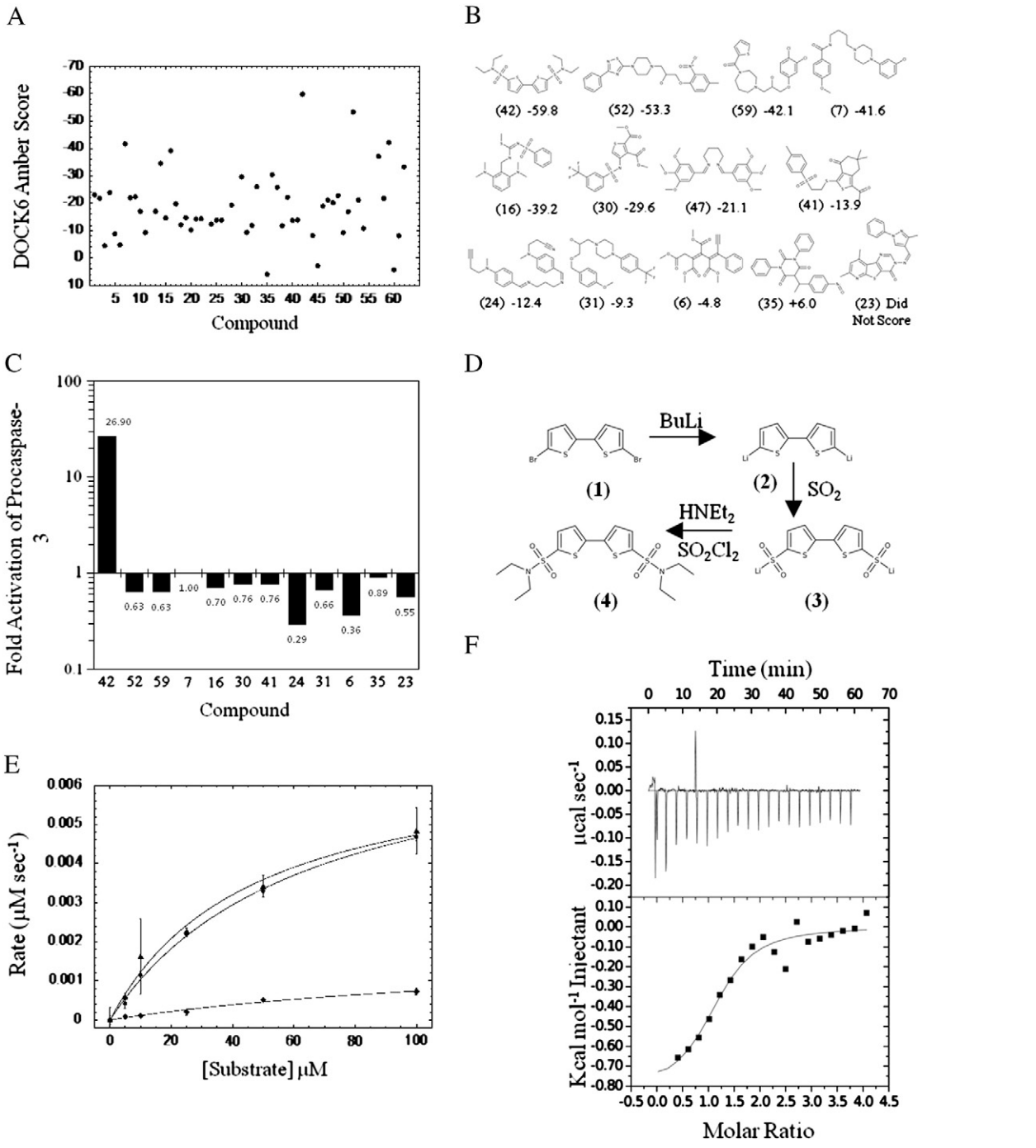

Fig. 4. Compound binding to procaspase-3. (A) Scores obtained from docking sixty-two compounds to the interface of caspase-3. (B) Structures of thirteen compounds tested as potential activators. Numbers in parentheses correspond to the compound number in panel A, and docking scores are shown next to the compound number. (C) Activity of procaspase-3 in the presence of twelve compounds from panel B. Note that compound 47 was insoluble in DMSO so was not tested further. (D) Overall synthesis scheme for compound 42. n-Butyllithium is added to 5,5′-dibromo-2,2′-bithiophene (**1**) to yield the bi-lithium derivative (**2**). Addition of sulfur dioxide to derivative **2** yields the sulfonyl bithiophene derivative (**3**). Addition of sulfuryl chloride and diethylamine to compound **3** yields the product (**4**). (E) Activity of procaspase-3 in the presence of various concentrations of compound 42. Catalytic parameters (K_M, k_{cat}, k_{cat}/K_M) determined from the data are described in the text. Purchased (closed triangles) and synthesized (closed circles) compound 42 gave the same results. The activity of procaspase-3 in the absence of compound is shown as closed diamonds. (F) Binding of compound 42 to caspase-3 measured by isothermal titration calorimetry. Upper panel shows raw ITC data from 20 injections of compound (2 μL of a 500 μM solution) into protein (50 μM). Lower panel shows the titration curve as a plot of energy exchanged (in kcal mol^{-1} of injectant) compared to the molar ratio of compound-to-protein.

assays. The thirteen compounds encompass a range of docking scores and poses, from predicted good binders (compound 42, for example) to predicted poor binders (compound 35, for example), as the goal of the work is to identify potential scaffolds from which structure–activity relationship (SAR) studies can be performed to generate libraries of compounds. One compound was not soluble in DMSO, so twelve compounds ultimately were used in activity studies.

3.2. Procaspase-3 activity in presence of compounds

The activity of procaspase-3 was examined in the presence of the compounds, where the compound concentration varied from 200 nM to 400 μM. Higher concentrations were impractical due to the solubility in DMSO for many of the compounds. The results showed that one of the molecules (compound 42) resulted in 27-fold increase

in substrate cleavage by procaspase-3 at higher concentrations (Fig. 4C). The remaining compounds either had no effect on activity or were somewhat inhibitory. Compound 42 is a sulphonyl bithiophene derivative, and we devised a scheme to synthesize the compound (see Section 2.3 and Fig. 4D).

The compound was used further in activity measurements of procaspase-3 to examine catalytic parameters of the enzyme (Fig. 4E). Procaspase-3 has very low enzyme activity that increases about 200-fold upon activation by IL cleavage [40]. While the zymogen appears to bind substrate equivalently to the mature enzyme, the catalytic efficiency is compromised. In the presence of 400 μM compound 42, the K_M, k_{cat} and k_{cat}/K_M values of procaspase-3 were determined to be 57 μM, 0.018 s^{-1}, and 316 M^{-1} s^{-1}, respectively. We note that there was no difference in the values when using compound purchased from vendor *versus* the compound synthesized in-house (Fig. 4E). A comparison of the catalytic parameters to those of procaspase-3 (K_M = ~44 μM; k_{cat} = 0.003 s^{-1}; k_{cat}/K_M = ~70 M^{-1} s^{-1}) shows that the compound has little effect on K_M but increases the catalytic efficiency of the enzyme about 6-fold. After removal of the compound through dialysis, the increase in activity was lost, indicating that this reaction is reversible (data not shown). It was interesting to note that while compound 42 increased the activity of procaspase-3, the rate of substrate cleavage by mature caspase-3 was unchanged in the presence of 400 μM compound 42 (data not shown).

The results can be compared to an activator of procaspase-3 previously described by Wells and coworkers [41]. Called compound 1541, the substituted phenyl-imidazopyridine-methoxy coumarin derivative demonstrated about 57-fold increase in k_{cat}/K_M compared to that of procaspase-3, where the k_{cat} was 0.016 s^{-1} and K_M was 14 μM upon incubation with the compound. While the enzyme efficiency is similar when activated by compound 1541 or compound 42, a significant difference is observed in the EC_{50}. For the coumarin derivative, an EC_{50} of 2.4 μM was reported [41], whereas the sulphonyl bithiophene derivative reported here has an EC_{50} in the high micromolar range. We note that at this point it is difficult to compare the two compounds directly since the previous study used wild-type procaspase-3, and incubation with compound 1541 resulted in self-activation of the zymogen via cleavage of the IL. In the studies presented here, we have used an uncleavable variant of procaspase-3 in order to focus on the conformational change in the zymogen that produces the active conformer. In addition, the enzymatic parameters determined by Wells' group were reported for a different substrate, IETD-AFC *versus* DEVD-AFC used here. Consequently, further studies are necessary to directly compare the mechanisms of the two compounds.

The binding of compound 42 to caspase-3 was examined by isothermal titration calorimetry (ITC). The data show that the reaction is exothermic, and a single molecule binds with a K_D of ~4 μM (Fig. 4F). Even at high protein concentrations (50 μM) and with compound concentration at ten times that of the protein, the ensuing signal was low, indicative of low enthalpy binding. We note that Brandts and coworkers [42] showed that for accurate identification of the thermodynamic properties, the product, c, of the K_a and the protein concentration should be between 1 and 1000. In our experiments, c was ~6, which is at the very low end of that range. Increasing the concentration of the protein and compound to further increase c, and therefore the sensitivity, was not possible because the poor solubility of compound 42 required an increase in the final concentration of DMSO, which also compromised protein structure.

With those caveats in mind, a number of useful conclusions can still be obtained from these data. The observed ΔH of ~−760 cal mol^{-1} is less than that of one hydrogen bond. However, with the TΔS calculated to be 6.8 kcal mol^{-1}, we can conclude that compound binding is entropically rather than enthalpically driven. The calculated stoichiometry of one molecule binding per dimer is consistent with compound binding in the dimer interface (duplicate experiments showed $n = 1.16 \pm 0.11$). Due to the symmetrical nature of the protein, a stoichiometry of $n = 2$ would be expected for molecules that bind elsewhere, as is observed, for example, with inhibitors that bind to the active site. We also observed that ITC experiments performed on a caspase-3 mutant, V266K, showed no binding of compound 42 (data not shown). The relatively bulky lysine residues in the center of the dimer interface would prevent the binding of the compound as proposed. The mutant is fully active, and the x-ray crystal structure shows little to no change compared to wild-type caspase-3 (J. Maciag and A. C. Clark, unpublished data), so other possible sites of binding should be unaffected by the mutation, and such interaction should be observed by ITC. Overall, the lack of binding to the V266K variant is consistent with compound 42 binding in the dimer interface.

While the ITC data indicated a K_D in the low micromolar range for the binding of compound 42 to caspase-3, no increase in substrate cleavage by procaspase-3 was observed below 50 μM compound, indicating the EC_{50} is likely in the high micromolar range for procaspase-3. The same ITC experiment was performed with procaspase-3; however, no signal was observed. It is possible that the presence of the intact ILs in the zymogen, which covers the dimer interface, significantly reduces the binding affinity. In conjunction with a low heat of binding, the overall effect may make detection of compound 42 binding to procaspase-3 by ITC difficult. It is also probable that the binding of the compound results in the loss of the network of water molecules that link the R164 side-chains from each monomer across the dimer interface. The displacement of constrained waters without replacing those hydrogen bonds likely offsets other favorable enthalpic contributions, resulting in the observed low binding heat. Together, these events may result in the observed weak activation of procaspase-3. The bridge of water molecules stabilizes the intercalated arginine residues in the interface, and is present in both active caspase-3 and the active V266E variant [13]. Loss of the water network, and its stabilizing interactions with R164, could also explain the difference observed between the binding affinity (~4 μM) and the EC_{50} (high micromolar) for compound 42.

We note that in the enzyme activity assays, the zymogen was incubated with compound for approximately one hour prior to activity measurements, which appears to be sufficient to convert the procaspase to the active conformer. We suggest that using the cleaved form of caspase-3 in ITC studies yields valuable information because our goal is to identify compounds that bind to and stabilize the active conformation found in the dimer interface. We have suggested that the interfaces are identical for both the cleaved caspase-3 and the active procaspase-3 [13], with the exception of the intact IL in the zymogen. Overall, the data further highlight the necessity for finding lead compounds with significantly greater stabilization of the active conformation than that observed for compound 42 through an increase in the enthalpic contribution and favorable interactions with the R164 residues.

3.3. Potential mode of binding in the interface

The dimer interface of caspase-3 contains a water-filled cavity of approximate dimensions 20 Å × 13 Å × 13 Å (L × W × H), where V266 is located at the bottom of the cavity (Fig. 5A). Docking poses of compound 42 indicate that it binds in the same region of the interface as the IL of the zymogen, presumably shifting procaspase-3 to the active conformer by expelling the IL from the interface. The compound potentially H-bonds with Y197 of both monomers, although there appear to be no interactions between the scaffold and R164 (Fig. 5B). The ability of the compound to form only one to two H-bonds is consistent with the low binding enthalpy observed by ITC (Fig. 4). In addition, the diethyl moieties on one side of the molecule face the hydrophobic cavity, whereas on the other side they lie along the surface of the cavity (Fig. 5B,C). In both cases, the groups form favorable hydrophobic contacts in the interface. A surface

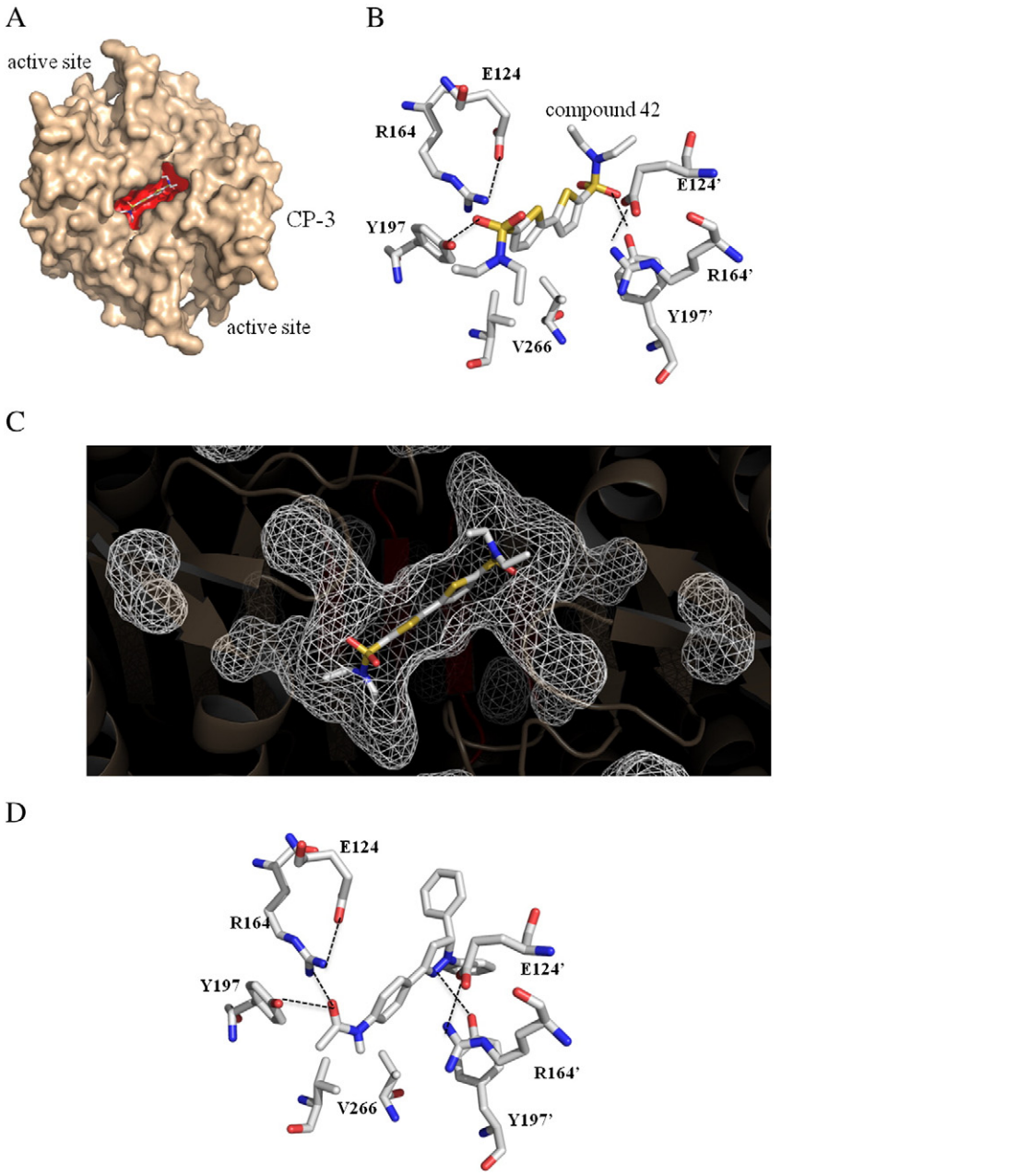

Fig. 5. Docking of activators to procaspase-3 interface. (A) Surface view of caspase-3 highlighting the dimer interface (red). The two active sites are labeled, and the protein is in the same orientation as in Fig. 1A. (B) Docking of compound 42 to the dimer interface. The compound can form hydrogen bonds with Y197 from both monomers, but there are no interactions with R164. (C) Surface representation of the interface cavity demonstrating the unfilled space when bound by compound 42. (D) Potential activator identified in a high-throughput screen (AID: 463141) for procaspase-3 activators (IUPAC: N-[4-(2,3,-diphenyl-3,4-dihydropyrazol-5-yl)phenyl]acetamide; SID: 49647539; CID: 3292253). Docking of the compound to the dimer interface shows potential interactions between Y197 and R164 from both monomers.

representation shows that the cavity extends away from the interface laterally to the neighboring β-strands. Several regions of the cavity are not filled by compound 42 (Fig. 5C), suggesting that binding to the cavity can be optimized with moieties other than the diethyl groups. Overall, the data suggest that although compound 42 activates procaspase-3 by preventing the IL from binding in the interface, it does so weakly due to poor optimization to the binding surface as well as lack of H-bonding potential to key residues in the dimer interface.

In order to examine the potential of other scaffolds as procaspase-3 activators, we searched the PubChem Bioassay database for activators identified by high-throughput screening methods. One assay (AID: 463141) [43] from the Scripps Research Institute Molecular Screening Center reported the identification and development of several probes as activators of procaspase-3. The assay utilized the uncleavable procaspase-3 variant described here, examined 326,028 compounds for activation of the zymogen, and identified approximately 300 potential activators. The probe that demonstrated the highest activity in the HTS assay is shown in Fig. 5D. The compound is a phenyl-acetamide derivative, and the chemical structure information for this probe is available in the PubChem Substance and Compound database (substance identifier number SID: 49647539; chemical structure identifier CID: 3292253) [44,45]. While at present the mechanism by which the compound activates procaspase-3 is unknown, we examined the potential of the compound to bind to the caspase-3 interface cavity. Docking studies showed that not only would binding of the compound to the interface displace the IL, but

the compound also can potentially hydrogen bond to R164 as well as Y197 (Fig. 5D). The preliminary data from the PubChem database suggests that the compound binds to the zymogen with much higher affinity than described here for compound 42 since the concentration of probes used in the assay was <10 μM. Hence, there appear to be a number of scaffolds that potentially can bind in the interface to displace the IL as well as form multiple H-bonds with the critical residues R164 and Y197, stabilizing the active site loops.

Overall, the collective data from Wells [41], the results described here, and results of compounds identified through HTS assays demonstrate that procaspase-3 can be activated either through a conformational change to stabilize an active conformer or through self-cleavage, although we note that the two mechanisms are not mutually exclusive. As shown previously [13,31,41], the activated procaspase efficiently kills cancer cells. In principle, compounds may act by binding to the protein surface and stabilizing the active site loops in the "on" state, but the most likely mechanism utilizes the allosteric site in the dimer interface. In this way, multiple active site loops can be stabilized in a single site. The identification of allosteric activators of procaspase-3 as a new therapeutic strategy in the treatment of cancer appears promising based on our current understanding of the activation process.

4. Conclusions

The allosteric site in the dimer interface of caspase-3 is bifunctional, where the active or inactive conformers are accessible and can be stabilized depending on the context of the protein. In the mature caspase-3, the binding of allosteric inhibitors to the interface results in an order-to-disorder transition in the active site loops. In procaspase-3, by contrast, where the equilibrium favors the inactive conformer, we propose that the binding of allosteric activators to the interface results in a disorder-to-order transition in the active site loops. The data presented here suggest two basic requirements for efficient activation of procaspase-3 using the allosteric site of the interface. First, the compound should optimize van der Waals contacts while expelling the intersubunit linker from binding in the same site. Second, the scaffold should form hydrogen bonds with R164 and Y197 (and possibly E124) to lock the active site loops in the "on" state as well as replace the interactions from a conserved water network, maintaining favorable enthalpic contributions. In this way, the activator binds efficiently to the protein and stabilizes the active conformer.

The results presented here demonstrate that targeting the dimer interface of procaspase-3 as a novel allosteric site for enzyme activation may be a viable target for the treatment of cancer. Compound 42 weakly activates procaspase-3, yet these studies suggest changes in the scaffold for improved interactions to increase compound potency. Such studies are an important step in the drug design process where future directions for increasing drug effectiveness are not often obvious. Even if a disease target is identified and well characterized, the identification of a compound that efficiently induces the desired effect can be a long and expensive journey. Although high throughput screening plays an important role in the discovery of lead compounds, an understanding of the thermodynamics involved, beyond the binding strength, is often crucial for making the transition to an effective and successful drug. The optimization of HIV-1 protease inhibitors is a prime example. Freire and coworkers showed that the first generation of inhibitors were entropically driven, often accompanied by an unfavorable enthalpic penalty [46,47]. This realization led to a shift in design to increase the enthalpy of binding, resulting in the creation of the next generation of protease inhibitors with dramatically improved effectiveness. A number of excellent reviews are available that further discuss the importance of thermodynamics and drug discovery [48–50].

Supplementary materials related to this article can be found online at doi:10.1016/j.bpc.2011.05.013.

Acknowledgments

The authors thank Dr. Ashutosh Tripathy (UNC Macromolecular Interactions Facility) and Dr. Hanna Gracz (NCSU Molecular and Structural Biochemistry) for assistance with ITC and NMR experiments, respectively. This work was supported by a grant from the National Institutes of Health (GM065970 to A.C.C.).

References

[1] A.G. Renehan, C. Booth, C.S. Potten, What is apoptosis, and why is it important? British Medical Journal 322 (2001) 1536–1538.
[2] A.L. Edinger, C.B. Thompson, Death by design: apoptosis, necrosis and autophagy, Current Opinion in Cell Biology 16 (2004) 663–669.
[3] M.C. Maiuri, E. Zalckvar, A. Kimchi, G. Kroemer, Self-eating and self-killing: crosstalk between autophagy and apoptosis, Molecular Cell Biology 8 (2007) 741–752.
[4] S.J. Riedl, G.S. Salvesen, The apoptosome: signalling platform of cell death, Molecular Cell Biology 8 (2007) 405–413.
[5] M.A. Hughes, N. Harper, M. Butterworth, K. Cain, G.M. Cohen, M. MacFarlane, Reconstitution of the death-inducing signaling complex reveals a substrate switch that determines CD95-mediated death or survival, Molecular Cell 35 (2009) 265–279.
[6] K.M. Boatright, G.S. Salvesen, Mechanisms of caspase activation, Current Opinion in Cell Biology 15 (2003) 725–731.
[7] Y. Shi, Mechanisms of caspase activation and inhibition during apoptosis, Molecular Cell 9 (2002) 459–470.
[8] S.H. MacKenzie, A.C. Clark, Targeting cell death in tumors by activating caspases, Current Cancer Drug Targets 8 (2008) 98–109.
[9] C. Pop, G.S. Salvesen, Human caspases: activation, specificity, and regulation, Journal of Biological Chemistry 33 (2009) 21777–21781.
[10] D. Datta, J.M. Scheer, M.J. Romanowski, J.A. Wells, An allosteric circuit in caspase-1, Journal of Molecular Biology 381 (2008) 1157–1167.
[11] J.M. Scheer, M.J. Romanowski, J.A. Wells, A common allosteric site and mechanism in caspases, Proceedings of the National Academy of Sciences USA 103 (2006) 7595–7600.
[12] J.A. Hardy, J. Lam, J.T. Nguyen, T. O'Brien, J.A. Wells, Discovery of an allosteric site in the caspases, Proceedings of the National Academy of Sciences USA 101 (2004) 12461–12466.
[13] J. Walters, C. Pop, F.L. Scott, M. Drag, P. Swartz, C. Mattos, G.S. Salvesen, A.C. Clark, A consitutively active and uninhibitable caspase-3 zymogen efficiently induces apoptosis, Biochemical Journal 424 (2009) 335–345.
[14] K.M. Boatright, M. Renatus, F.L. Scott, S. Sperandio, H. Shin, I.M. Pedersen, J.-E. Ricci, W.A. Edris, D.P. Sutherlin, D.R. Green, G. Salvesen, A unified model for apical caspase activation, Molecular Cell 11 (2003) 529–541.
[15] C. Pop, P. Fitzgerald, D.R. Green, G.S. Salvesen, Role of proteolysis in caspase-8 activation and stabilization, Biochemistry 46 (2007) 4398–4407.
[16] M.L. Wurstle, M.A. Laussmann, M. Rehm, The caspase-8 dimerization/dissociation balance is a highly potent regulator of caspase-8, -3, -6 signaling, Journal of Biological Chemistry 285 (2010) 33209–33218.
[17] C. Pop, J. Timmer, S. Sperandio, G.S. Salvesen, The apoptosome activates caspase-9 by dimerization, Molecular Cell 22 (2006) 269–275.
[18] A. Oberst, C. Pop, A.G. Tremblay, V. Blais, J.-B. Denault, G.S. Salvesen, D.R. Green, Inducible dimerization and inducible cleavage reveal a requirement for both processes in caspase-8 activation, Journal of Biological Chemistry 285 (2010) 16632–16642.
[19] C. Pop, Y.-R. Chen, B. Smith, K. Bose, B. Bobay, A. Tripathy, S. Franzen, A.C. Clark, Removal of the pro-domain does not affect the conformation of the procaspase-3 dimer, Biochemistry 40 (2001) 14224–14235.
[20] W.A. Witkowski, J.A. Hardy, L2' loop is critical for caspase-7 active site formation, Protein Science 18 (2009) 1459–1468.
[21] J.A. Hardy, J.A. Wells, Dissecting an allosteric switch in caspase-7 using chemical and mutational probes, Journal of Biological Chemistry 284 (2009) 26063–26069.
[22] Z.F. Gellad, D. Provenazle, Colorectal cancer: national and international perspective on the burden of disease and public health impact, Gastroenterology 138 (2010) 2177–2190.
[23] A.F. Kabore, J.B. Johnston, S.B. Gibson, Changes in the apoptotic and survival signaling in cancer cells and their potential therapeutic implications, Current Cancer Drug Targets 4 (2004) 147–163.
[24] S. Fulda, K.-M. Debatin, Targeting apoptosis pathways in cancer therapy, Current Cancer Drug Targets 4 (2004) 569–576.
[25] X.W. Meng, S.-H. Lee, S.H. Kaufmann, Apoptosis in the treatment of cancer: a promise kept? Current Opinion in Cell Biology 18 (2006) 668–676.
[26] T.-T. Tan, E. White, Therapeutic targeting of death pathways in cancer: mechanisms for activating cell death in cancer cells, in: R. Khosravi-Far, E. White (Eds.), Programmed Cell Death in Cancer Progression, Springer, Philadelphia, 2008, pp. 81–104.
[27] S. Fulda, Caspase-8 in cancer biology and therapy, Cancer Letters 281 (2009) 128–133.
[28] B. Pennarun, A. Meijer, E.G.E. de Vries, J.H. Kleibeuker, F. Kruyt, S. de Jong, Playing the DISC: turning on TRAIL death receptor-mediated apoptosis in cancer, Biochemica et Biophysica Acta 1805 (2010) 123–140.
[29] H.-G. Zhang, J. Wang, X. Yang, H.-C. Hsu, J.D. Mountz, Regulation of apoptosis proteins in cancer cells by ubiquitin, Oncogene 23 (2004) 2009–2015.

[30] S. Fulda, Tumor resistance to apoptosis, International Journal of Cancer 124 (2009) 511–515.
[31] K.S. Putt, G.W. Chen, J.M. Pearson, J.S. Sandhorst, M.S. Hoagland, J.-T. Kwon, S.-K. Hwang, H. Jin, M.I. Churchwell, H.-H. Cho, D.R. Doerge, W.G. Helferich, P.J. Hergenrother, Small-molecule activation of procaspase-3 to caspase-3 as a personalized anticancer strategy, Nature Chemical Biology 2 (2006) 543–550.
[32] G.K. Ackers, D.W. Bolen, The Gibbs conference on biothermodynamics: origins and evolution, Biophysical Chemistry 64 (1997) 3–5.
[33] P.T. Lang, D. Moustakas, S. Brozell, N. Carrascal, S. Mukherjee, S. Pegg, K. Raha, D. Shivakumar, R. Rizzo, D. Case, B. Shoichet, I. Kuntz, DOCK, Version 6.3, University of California, San Francisco, USA, 2009.
[34] A.P. Graves, D.M. Shivakumar, S.E. Boyce, M.P. Jacobson, D.A. Case, B.K. Shoichet, Rescoring docking hit lists for model cavity sites: predictions and experimental testing, Journal of Molecular Biology 377 (2008) 914–934.
[35] E.F. Petersen, T.D. Goddard, C.C. Huang, G.S. Couch, D.M. Greenblatt, E.C. Meng, T.E. Ferrin, UCSF Chimera — a visualization system for exploratory research and analysis, Journal of Computational Chemistry 25 (2004) 1605–1612.
[36] K. Bose, C. Pop, B. Feeney, A.C. Clark, An uncleavable procaspase-3 mutant has a lower catalytic efficiency but an active site similar to that of mature caspase-3, Biochemistry 42 (2003) 12298–12310.
[37] B. Feeney, C. Pop, A. Tripathy, A.C. Clark, Ionic interactions near loop L4 are important for maintaining the active site environment and the dimer stability of (pro)caspase-3, Biochemical Journal 384 (2004) 515–525.
[38] B. Feeney, A.C. Clark, Reassembly of active caspase-3 is facilitated by the propeptide, Journal of Biological Chemistry 280 (2005) 39772–39785.
[39] C.A. Lipinski, F. Lombardo, B.W. Dominy, P.J. Feeney, Experimental and computational approaches to estimate solubility and permeability in drug discovery and development settings, Advanced Drug Delivery Reviews 46 (2001) 3–26.
[40] C. Pop, B. Feeney, A. Tripathy, A.C. Clark, Mutations in the procaspase-3 dimer interface affect the activity of the zymogen, Biochemistry 42 (2003) 12311–12320.
[41] D.W. Wolan, J.A. Zorn, D.C. Gray, J.A. Wells, Small-molecule activators of a proenzyme, Science 326 (2009) 853–858.
[42] T. Wiseman, S. Williston, J.F. Brandts, L. Lung-Nan, Rapid measurement of binding constants and heats of binding using a new titration calorimeter, Analytical Biochemistry 179 (1989) 131–137.
[43] National Center for Biotechnology Information. PubChem BioAssay Database; AID = 463141, Source = Scripps Research Institute Molecular Screening Center, http://pubchem.ncbi.nlm.nih.gov/assay/assay.cgi?aid=463141.
[44] National Center for Biotechnology Information. PubChem Substance Database; SID = 49647539, Source = Scripps Research Institute Molecular Screening Center, http://pubchem.ncbi.nlm.nih.gov/summary/summary.cgi?sid=49647539.
[45] N.C.f.B. Information, National Center for Biotechnology Information. PubChem Compound Database; CID = 3292253, http://pubchem.ncbi.nlm.nih.gov/summary/summary.cgi?cid=3292253.
[46] H. Ohtaka, S. Muzammil, A. Schon, A. Vaelazquez-Campoy, S. Vega, E. Friere, Thermodynamic rules for the design of high affinity HIV-1 protease inhibitors with adaptability to mutations and high selectivity towards unwanted targets, International Journal of Biochemistry and Cell Biology 36 (2004) 1787–1789.
[47] A. Velazquez-Campoy, M.J. Todd, E. Friere, HIV-1 protease inhibitors: enthalpic versus entropic optimization of the binding affinity, Biochemistry 39 (2000) 2201–2207.
[48] P.D. Ross, S. Subramanian, Thermodynamics of protein association reactions: forces contributing to stability, Biochemistry 20 (1981) 3096–3102.
[49] J.B. Chaires, Calorimetry and thermodynamics in drug design, Annual review of biophysics 37 (2008) 135–151.
[50] E. Friere, Do enthalpy and entropy distinguish first in class from best in class? Drug Discovery Today 13 (2008) 869–874.